Characterization of poroelastic materials with a bayesian approach

Jean-Daniel Chazot, Jérôme Antoni, Erliang E. Zhang

▶ **To cite this version:**

Jean-Daniel Chazot, Jérôme Antoni, Erliang E. Zhang. Characterization of poroelastic materials with a bayesian approach. 10ème Congrès Français d'Acoustique, Apr 2010, Lyon, France. hal-00554439

HAL Id: hal-00554439
https://hal.science/hal-00554439v1

Submitted on 10 Jan 2011

HAL is a multi-disciplinary open access archive for the deposit and dissemination of scientific research documents, whether they are published or not. The documents may come from teaching and research institutions in France or abroad, or from public or private research centers.

L'archive ouverte pluridisciplinaire **HAL**, est destinée au dépôt et à la diffusion de documents scientifiques de niveau recherche, publiés ou non, émanant des établissements d'enseignement et de recherche français ou étrangers, des laboratoires publics ou privés.

10ème **C**ongrès **F**rançais d'**A**coustique

Lyon, 12-16 Avril 2010

Characterization of poroelastic materials with a bayesian approach

Jean-Daniel Chazot, Jérôme Antoni, Erliang Zhang

Université de Technologie de Compiègne, CNRS UMR 6253 Roberval, 60205 Compiègne Cedex, France, jean-daniel.chazot@utc.fr

A characterization method of poroelastic intrinsic parameters is used and compared with other direct methods. This inverse characterization method enables to get all the parameters with a simple measurement in a standing wave tube. It is based on a bayesian approach that enables to get probabilistic data such as the maximum aposteriori value and confidence intervals on each parameter. In this approach, it is necessary to define prior information on the parameters depending on the studied material. This last point is very important to regularize the inverse problem of identification. In a first step, the direct problem formulation is presented. Then, the inverse characterization is developed and applied to an experimental case.

1 Introduction

Sound insulation of various structures with porous materials finds its interest in several industrial domains such as building acoustics, automotive, and aeronautics. It is therefore important, at design stage, to be able to characterize the vibroacoustic behavior of these poroelastic structures. In practice Biot's model[1] is commonly used. However eight parameters are necessary to describe the poroelastic material. Several kinds of characterization, direct or not, can be used to get acoustical parameters [9, 5, 12] or elastic parameters of the solid phase [7, 14, 2, 8]. However these kinds of characterisation measurements require a specific experimental device for each parameter. Besides, uncertainties obtained on each measurement are sometimes very large and lead to some difficulties to get a good comparison of the model with standard experimental data obtained with a standing wave tube apparatus. Finally, for particular materials like fibrous ones, some parameters like elastic coefficients are very difficult to identify even with direct methods. The non-linear dynamic behavior is indeed well known for such materials where the apparent stiffeness depends on the strain level at which the sample is tested [13]. On the other hand, inverse acoustic measurements [6, 3, 4] as well as indirect methods [11, 10] can also be used to adjust these parameters.

In this paper, a robust inverse method is presented. All the parameters, acoustic and elastic, are characterised with only one measurement in a standing wave tube. The baysian theory is used to improve the efficiency of the optimisation scheme to identify the parameters. The resulting cost function is therefore a combination of the likelihood function and the prior information. Estimated values of the parameters are obtained via a minimisation of the cost function performed with a global search and a refined local search. Descent optimisation methods and MCMC methods have hence been tested with simulated data and have led to very good results. One interesting feature of the MCMC method is to get the probability density functions of each parameter as well as the joint probability density functions between parameters. Uncertainties can hence be given on estimated values of each parameter as well as dependencies between parameters.

2 Poroelastic model description

The Biot's model presented in this paper is used to calculate the reflexion and transmission coefficients of a porous material sample in a standing wave tube. Knowing these coefficients it is possible to predict the pressure at any position inside the tube.

2.1 Biot's model

In Biot's theory, poroelastic materials are defined as materials consisting of a fluid and a solid phase. Biot's model takes into account three different interactions between the two phases.

Elastic coupling is taken into account in Equ. 1:

$$\left\{ \begin{array}{l} \boldsymbol{\sigma}^s = 2N\ \boldsymbol{\varepsilon}^s + (P-2N)\ \mathrm{tr}(\boldsymbol{\varepsilon}^s)\ \mathbf{I} + Q\ \mathrm{tr}(\boldsymbol{\varepsilon}^f)\ \mathbf{I}\ , \\ \boldsymbol{\sigma}^f = R\ \mathrm{tr}(\boldsymbol{\varepsilon}^f)\ \mathbf{I} + Q\ \mathrm{tr}(\boldsymbol{\varepsilon}^s)\ \mathbf{I}\ , \end{array} \right. \tag{1}$$

where $\boldsymbol{\sigma}^s$ (resp. $\boldsymbol{\sigma}^f$) represents the solid (resp. fluid) stress tensor, and $\boldsymbol{\varepsilon}^s$ (resp. $\boldsymbol{\varepsilon}^f$) represents the solid (resp. fluid) strain tensor. $\mathbf{I}$ is the identity matrix, and P,Q,R, and N are classical elastic coefficients used in Biot's model and detailed in Equ. 2.

$$\begin{aligned} P &= \frac{4}{3}N + K_b + \frac{(1-\phi)^2}{\phi}K_f\ , \\ Q &= \frac{R(1-\phi)}{\phi}\ , \\ R &= \phi K_f\ . \end{aligned} \tag{2}$$

N, K_b and ρ_s are respectively the shear modulus, the bulk modulus and the density of the solid frame. ϕ is the porisity, and K_f is the fluid compressibility

modulus.

Inertial coupling is taken into account in Equ. 3:

$$\begin{cases} \vec{\text{div}}(\boldsymbol{\sigma}^s) = \rho_{11}\,\vec{\boldsymbol{\gamma}}^s + \rho_{12}\,\vec{\boldsymbol{\gamma}}^f \ , \\ \vec{\text{div}}(\boldsymbol{\sigma}^f) = \rho_{22}\,\vec{\boldsymbol{\gamma}}^f + \rho_{12}\,\vec{\boldsymbol{\gamma}}^s \ , \end{cases} \tag{3}$$

where ρ_{11},ρ_{22}, and ρ_{12} are the classical inertial coupling coefficients used in Biot's model given in reference, and recalled in Equ. 4.

$$\begin{aligned} \rho_{11} &= \rho_s + \phi\rho_f - \phi\rho_0 \ , \\ \rho_{12} &= -\phi\rho_f + \phi\rho_0 \ , \\ \rho_{22} &= \phi\rho_f \ . \end{aligned} \tag{4}$$

Viscous and thermal dissipations are respectively taken into account by frequency-dependant expressions of fluid density ρ_f and dynamic fluid compressibility K_f. Johnson-Allard's expressions, given with a time dependence $e^{-j\omega t}$ in Equ. 5, are used to describe the micro-geometry structure with five parameters : porosity ϕ , tortuosity α_∞ , airflow resistivity σ, and viscous and thermal characteristic lengths Λ and Λ'. The airflow resistivity can also be related to the viscous permeability with $\sigma = \eta/k_0$ where η is the dynamic fluid viscosity. Pr is the Prandtl number.

$$\begin{aligned} \rho_f &= \rho_0\alpha_\infty\left(1 - \frac{\sigma\phi}{j\rho_0\alpha_\infty\omega}\sqrt{1 - 4j\frac{\eta\alpha_\infty^2\omega\rho_0}{\Lambda^2\phi^2\sigma^2}}\right) \\ K_f &= \frac{\gamma P_0}{\gamma - (\gamma-1)\left(1 - \frac{8\eta}{j\Lambda'^2\,\mathrm{Pr}\,\omega\rho_0}\sqrt{1 - j\rho_0\frac{\mathrm{Pr}\,\Lambda'^2\omega}{16\eta}}\right)^{-1}} \end{aligned} \tag{5}$$

2.2 Standing wave tube

The case of a poroelastic material sample placed in a standing wave tube and submitted to a normal incident plane wave is considered as depicted in Fig. 1. The reduced one-dimensional Biot's model is therefore employed. In this case, the shear wave is not present in the poroelastic material. Only the solid and fluid compressional waves are necessary to take into account. Using the wave formalism, the fluid and solid displacements can hence be obtained as deriving from two scalar potentials:

$$\begin{aligned} \vec{\mathbf{U}}_s &= \boldsymbol{\nabla}\left(Ae^{jk_1x} + Be^{-jk_1x}\right) + \boldsymbol{\nabla}\left(Ce^{jk_2x} + De^{-jk_2x}\right) \\ \vec{\mathbf{U}}_f &= \mu_1\boldsymbol{\nabla}\left(Ae^{jk_1x} + Be^{-jk_1x}\right) + \mu_2\boldsymbol{\nabla}\left(Ce^{jk_2x} + De^{-jk_2x}\right) \end{aligned} \tag{6}$$

A time dependency $e^{-j\omega t}$ is chosen. Wave numbers k_1,k_2 and amplitude coefficients μ_1,μ_2 between the solid and fluid displacements are recalled in Equ. 7:

$$\begin{aligned} k_1 &= \sqrt{\tfrac{\omega^2}{2(PR-Q^2)}\left(P\rho_{22} + R\rho_{11} - 2Q\rho_{12} - \sqrt{\Delta}\right)}, \\ \mu_1 &= \tfrac{Pk_1^2 - \omega^2\rho_{11}}{\omega^2\rho_{12} - Qk_1^2}, \\ k_2 &= \sqrt{\tfrac{\omega^2}{2(PR-Q^2)}\left(P\rho_{22} + R\rho_{11} - 2Q\rho_{12} + \sqrt{\Delta}\right)}, \\ \mu_2 &= \tfrac{Pk_2^2 - \omega^2\rho_{11}}{\omega^2\rho_{12} - Qk_2^2}. \end{aligned} \tag{7}$$

with $\Delta = (P\rho_{22} + R\rho_{11} - 2Q\rho_{12})^2 - 4(PR-Q^2)(\rho_{11}\rho_{22} - \rho_{12}^2)$.

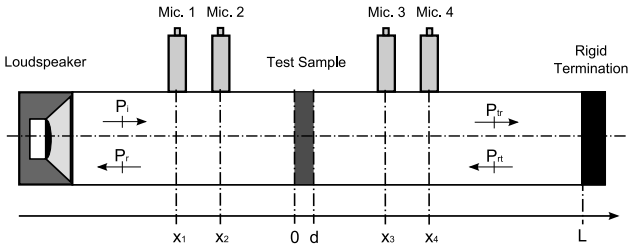

Figure 1: Standing-wave tube setup

Unknown amplitudes A, B, C and D are determined using the boundary conditions at the interface of the poroelastic material sample. In the present case of an acoustic-poroelastic interface, coupling conditions are given in Equ. 8. These equations are based on the flow, the fluid pressure, and the total normal stress continuity conditions.

$$\begin{cases} \phi\ \vec{\mathbf{V}}_f\ .\vec{\mathbf{n}} + (1-\phi)\ \vec{\mathbf{V}}_s\ .\vec{\mathbf{n}} = \vec{\mathbf{V}}_a\ .\vec{\mathbf{n}}\ , \\ \phi\ \boldsymbol{\sigma}^f.\vec{\mathbf{n}} + (1-\phi)\ \boldsymbol{\sigma}^s.\vec{\mathbf{n}} = -P_a.\vec{\mathbf{n}}\ , \\ \boldsymbol{\sigma}^f.\vec{\mathbf{n}} = -P_a.\vec{\mathbf{n}}\ . \end{cases} \tag{8}$$

The acoustic pressure P_a and acoustic velocity V_a are related to the incident and reflected waves at $x = 0$, and to the transmitted and backward waves at $x = d$. Besides, incident and reflected waves are related by the reflection coefficient, incident and transmitted waves by the transmission coefficient, and transmitted and backward waves are by the rigid boundary condition at $x = L$.

Using Equ. 6 with Equ. 8, it is thus possible to calculate the reflection and transmission coefficient of the porous material sample. Then the total acoustic pressure can be determined at any position in the tube, and in particular at the four microphone positions, by summing the incident and reflected waves in the upstream section and by summing the transmitted and the backward waves in the downstream section. The only remaining unknown to set is the incident pressure.

3 Baysian identification method

The central idea beyond the Bayesian approach is to build a cost function with endowed constraints from the aposteriori probability density function (pdf) of the parameters to be inferred. In contrast to other optimisation techniques, this will confer to the cost function a direct probabilistic interpretation: not only will its maximisation provide the most likely values of the parameters given the measured data – the so-called maximum aposteriori (MAP) estimates – but its shape will be truly indicative of the joint probability distribution of the estimated parameters as well. In particular it will give access to the full covariance matrix, a fundamental quantity to assess the variability of the estimates and their mutual correlations.

3.1 Cost function

Namely, let $\theta = \{\phi, \alpha_\infty, \sigma, \Lambda, k_\Lambda, \rho_1, P, \eta_s\}$ be the vector of parameters to be inferred and $p(\theta|P_{ik}, P_k^{inc})$ its pdf conditional to the observations of the four pressures $P_{ik} \equiv P_i(\omega_k)$, $i = 1, 2, 3, 4$, as returned by the microphones and the incident pressure $P_k^{inc} \equiv P_{inc}(\omega_k)$ at frequencies ω_k, $k \in \mathcal{F}$. This is the *aposteriori* pdf which reflects all the information that can be inferred on θ from the measured data. Now from Bayes'rule

$$p(\theta|P_{ik}, P_k^{inc}) \propto p(P_{ik}|\theta, P_k^{inc})p(\theta) \tag{9}$$

where $p(P_{ik}|\theta, P_k^{inc})$ is the likelihood and $p(\theta)$ is the *apriori* pdf of the parameters, both of which can be given closed-form expressions. In words, $p(P_{ik}|\theta, P_k^{inc})$ reflects the direct problem which, given the values of θ and $P_{inc}(\omega_k)$ can predict the data $P_i(\omega_k)$ – notwithstanding measurement noise and modeling errors – whereas $p(\theta)$ is the mechanism to assign weights to the values of θ before the experience – based either on the user's expertise or subjective judgment, or on strict physical constraints. The choice of the apriori pdf will be discussed in the next subsection. That of the likelihood proceeds as follows. Since the measured data are functionally related to the vector of parameters θ as

$$P_{ik} = \beta_{ik}(\theta)P_k^{inc} + N_{ik} \tag{10}$$

where $\beta_{ik}(\theta)$ is a deterministic function that embodies the direct model and where N_{ik} accounts for additive measurement noise, it results that $p(P_{ik}|\theta, P_k^{inc}) = p_N(P_{ik} - \beta_{ik}(\theta)P_k^{inc})$ with $p_N(\cdot)$ standing for the pdf of N_{ik}. Upon invoking the Central Limit Theorem applied to the Fourier Transform, it happens that under mild conditions $p_N(\cdot)$ tends to a (complex) Gaussian distribution. Hence, after further assuming that the measurement noise is uncorrelated across the microphones,

$$p(\theta|P_{ik}, P_k^{inc}) = p(\theta) \prod_{\omega_k \in \mathcal{F}} \frac{\exp\left(-\sum_{i=1}^4 \frac{|P_{ik} - \beta_{ik}(\theta)P_k^{inc}|^2}{\sigma_{ik}^2}\right)}{\pi \prod_{i=1}^4 \sigma_{ik}^2}. \tag{11}$$

This is the closed-form expression of the aposteriori pdf of the parameters θ which can ow be explored in a variety of ways. In the present work, the optimal values of the parameters are sought so as to maximise this expression or, more conveniently, so as to minimise its negative logarithm

$$J(\theta) = -\ln p(\theta) + \sum_{\omega_k \in \mathcal{F}} \sum_{i=1}^4 \frac{|P_{ik} - \beta_{ik}(\theta)P_k^{inc}|^2}{\sigma_{ik}^2}. \tag{12}$$

In doing so, one should keep in mind that P_k^{inc} is the first quantity to be inferred since it is not measured by the microphones. This is easily achieved analytically by setting the gradient of $J(\theta)$ w.r.t. P_k^{inc} to zero, thus giving

$$\hat{P}_k^{inc} = \frac{\sum_{i=1}^4 \beta_{ik}(\theta)^* P_{ik} \sigma_{ik}^{-2}}{\sum_{i=1}^4 |\beta_{ik}(\theta)|^2 \sigma_{ik}^{-2}} \tag{13}$$

which is to be used in place of P_k^{inc} in $J(\theta)$.

3.2 Prior information

The apriori density function $p(\theta)$ on the inferred parameters plays a central rôle in the bayesian approach. It is actually the mechanism by which the inverse problem is regularised, i.e. forced to find an unique and stable solution. As mentioned above, there are many possible choices $p(\theta)$ that may reflect the user's apriori on the problem. In the present study, a separable pdf $p(\theta) = \prod_i^8 p(\theta_i)$ was chosen, meaning that the parameters are *a priori* mutually independent. Then, for the sake of simplicity, each pdf $p(\theta_i)$ was modelled as a Chi2 distribution with "scale parameter" λ_i and number of degrees-of-freedom ν_i, viz.,

$$\ln p(\theta_i) = -(\lambda_i - 1)\ln(a_i\theta_i + b_i) + \frac{\nu_i}{2}(a_i\theta_i + b_i) + C \tag{14}$$

with C a constant to be neglected in $J(\theta)$. This naturally enforces a constraint of positivity ($a_i = 1$, $b_i = 0$) on parameters σ, Λ, ρ_1, P and η_s, and after a suitable change of variable ($a_i = \pm 1$, $b_i = \mp 1$), constraints of having $\phi \leq 1$, $\alpha_\infty > 1$ and $k_\Lambda \geq 1$. Moreover, the values of λ_i and ν_i may be tuned from their relations $\lambda_i = \mu_{\theta_i}^2/\sigma_{\theta_i}^2$ and $\nu_i = 2\mu_{\theta_i}/\sigma_{\theta_i}^2$ with the expected mean μ_{θ_i} and variance $\sigma_{\theta_i}^2$ of the parameter θ_i.

4 Poroelastic parameters characterization

4.1 Experimental data

The identification process described in this paper relies on pressure measurements P_{ik} made in a standing wave tube presented in Fig. 1. A small tube and a large tube are used in order to get a wide frequency band from 50Hz to 5500Hz. It is important here to reach high frequencies to get, if possible, the effects of all the parameters including the solid phase elastic parameters. A multisinus excitation is also used to verify the linearity of the measurement.

4.2 Optimisation method

The aim of the optimisation tools described here is to get a good estimation of each parameter with a robust method and as few as possible a time-consuming method. Besides, the major problem to avoid is to be trapped in a local minimum of the cost function. With descent optimisation methods, the result depends highly on the inital starting point. These methods are therefore generally used for local search to refine a solution obtained after a global search. However, global search methods like genetic algorithm or monte-carlo methods are very time consuming when the number of parameters to estimate is important and when the search space is large. In the following, two complementary optimisation methods are detailed.

4.2.1 Constrained optimisation problem

When using optimisation tools, global search and local search must be employed wittingly. First, a global search is used to limit the search space. The chosen method to explore the domain is an interior-reflective Newton method with random initial values generated over a large search space. However, in order to ensure

a good convergence in a limited time, prior information similar to those used in the cost function are also employed to generate the initial random values. Initial values of the porosity are for example generated with a normal distribution around the mean value used as apriori (0.96). However it is also important to not limit the search domain with a too narrow distribution. The distribution of random initial values must therefore be adapted for each parameters.

Moreover, some parameters such as the resistivity or the elastic coefficient have a very wide range of possible values. It is thus important to limit the search domain by defining an reasonable mean value and a limited search space for these parameters. The user knowledge on the studied material is indeed usefull in this case to say whether the material is considered as rigid or soft and whether the material is considered as resistive or not. A constant distribution can then be used to generate random values around these values. The search domain is hence limited around the mean value with a constant distribution probability.

Finally, two optimisation loops are used with the same constrained nonlinear optimisation function. The first one explores the global search space, and then the second loop refines the solution in a more limited search space.

4.2.2 Markov Chain Monte Carlo method

Markov Chain Monte Carlo (MCMC) techniques are often applied in optimisation problems when facing large dimensional search spaces. The basic idea of such optimisation tools is to generate random samples and to explore the search space with a Markov Chain designed to spend more time in the most important regions, ie. around the maximum of the cost function. This method gives access to the joint probability density function of the inferred parameters and is very usefull to assess the accuracy of the parameters estimates.

The main drawback of this method is the time of computation necessary to ensure a good convergence when the search space is too large. This time can be quite long but is not insurmountable.

5 Experimental results and comparison with direct measurements

In order to evaluate the efficiency and the robustness of the proposed identification method, pressure measurements P_{ik} have been made with fibrous and porous materials. For sake of conciseness only one material is presented to illustrate the method reliability. The chosen material is a low density fibrous material called MAT 1. The thickness of the sample tested is 15mm. This material was also characterized with direct measurements taken as reference (see Table 1).

The expected mean μ_{θ_i} and variance $\sigma^2_{\theta_i}$ of each parameter θ_i used in apriori pdf are adjusted. Hence, compared to other fibrous material such as rockwool or glasswool, this synthetic fibrous material has a low density, and a low rigidity. Mean values and standard deviations used in the probability density functions are given in Table 1.

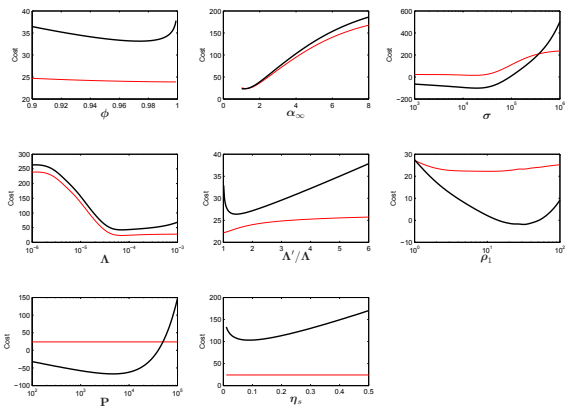

Figure 2: Cost Function evaluation - $f \in [400, 6000]$ with $\Delta f = 10Hz$ - Sample thickness : 1.5cm - Thick black line : cost function with prior information - thin red line : cost function without prior information

Table 1: Parameters.

Parameters	Mean Values	St.Dev.	MAT 1
ϕ	0.96	0.024	0.98
α_∞	1.15	2.5	1
σ $(10^3 Nm^{-4}s)$	31	8.4	21.2
Λ (μm)	98	59	60
k_Λ	2	0.58	1.7
ρ_1 (kg/m^3)	36	11	29
P $(10^3 Pa)$	5	1.4	6.6
η_s	0.093	0.019	0.13

The variance σ^2_{ik} on the measured pressures is also used to adjust the influence of the apriori information on the cost function. Its value is set to 5.10^{-3} and permits to take into account the measurement uncertainties but also the model uncertainties. Cost functions hence obtained are plotted in Fig. 2. Each parameters is tested around its mean value. One can observe here that apriori information are essential on some parameters that cannot be identified. This is the case for the solid phase parameters such as the elastic coefficient and the structural damping.

The aposteriori probability density functions (pdf) obtained with the MCMC method are presented on Fig. 3. The pdf of the solid density seems very flat. However, all the parameters can be infered from these pdf. The values obtained are presented and compared with direct measurements in Table 2. All the parameters are well identified, except the elastic coefficient and the structural damping. However, this material can be considered as a rigid frame material, and the solid phase elasticity is not taking part in the response measured by the microphones. It explains thus why the solid phase elastic coefficients cannot be well identified.

Table 2: Comparison with direct measurements.

Parameters	Reference	MCMC	Error %
ϕ	0.98	0.984	0.41
α_∞	1	1.01	1.1
σ $(10^3 Nm^{-4}s)$	21	19.4	8.7
Λ (μm)	60	62.9	4.8
k_Λ	1.7	1.74	4.2
ρ_1 (kg/m^3)	29	29.3	1.2
P $(10^3 Pa)$	6.6	4.2	30
η_s	0.13	0.008	38

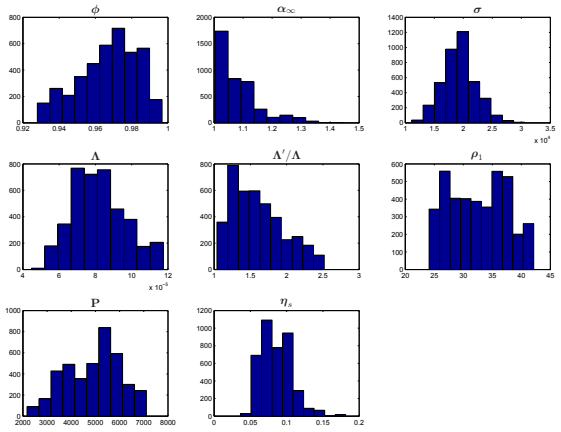

Figure 3: Probability density functions obtained with the MCMC method on material MAT 1

6 Conclusion

Descent optimisation methods and MCMC methods have hence been tested with experimental data and have led to good results. One interesting feature of the MCMC method is to get the probability density function of each parameter. Uncertainties can hence be given on estimated values of each parameter. It is however important to notice that apriori information on the material are very important. If apriori information are far from the reality, the cost function is less likely to find the real parameters and the starting initial values used in the optimisation method do not permit to ensure a good convergence toward the global minimum. Finally, it is also important to notice that several experimental data are necessary to get a good estimation of the parameters. Effects of circumferential edge constraint[13] and inhomogeneous material samples can hence be averaged over several samples.

Acknowledgments

The authors would like to thank Faurecia and Matelys for providing the materials used in this study.

References

[1] M.A. Biot. Generalized theory of acoustic propagation in porous dissipative media. *Journal of Acoustical Society of America*, 34(9):168–178, 1962.

[2] F. Chevillotte and R. Panneton. Elastic characterization of closed cell foams from impedance tube absorption tests. *Journal of Acoustical Society of America*, 122(5):2653–2660, 2007.

[3] T. Courtois, T. Falk, and C. Bertolini. An acoustical inverse measurement system to determine intrinsic parameters of porous samples. In *SAPEM*, ENTPE Lyon, 2005.

[4] R. Dragonetti, C. Ianniello, and R. Romano. The use of an optimization tool to search non-acoustic parameters of porous materials. In *Inter-noise*, Prague, 2004.

[5] Z.E.A. Fellah, M. Fellah, N. Sebaa, W. Lauriks, and C. Depollier. Measuring flow resistivity of porous materials at low frequencies range via acoustic transmitted waves (l). *Journal of Acoustical Society of America*, 119(4):1926–1928, 2006.

[6] G. Iannace, C. Ianiello, L. Maffei, and R. Romano. Characteristic impedance and complex wave-number of limestone chips. In *4th European Conference on Noise Control - Euronoise*, 2001.

[7] L. Jaouen, A. Renault, and M. Deverge. Elastic and damping characterizations of acoustical porous materials: Available experimental methods and applications to a melamine foam. *Applied Acoustics*, 69:1129–1140, 2008.

[8] C. Langlois, R. Panneton, and N. Atalla. Polynomial relations for quasi-static mechanical characterization of isotropic poroelastic materials. *Journal of Acoustical Society of America*, 122(5):2653–2660, 2007.

[9] W. Lauriks, L. Boeckx, P. Leclaire, P. Khurana, and L. Kelders. Characterisation of porous acoustic materials. In *SAPEM*, ENTPE Lyon, 2005.

[10] X. Olny and R. Panneton. Acoustical determination of the parameters governing thermal dissipation in porous media. *Journal of Acoustical Society of America*, 123(2):814–824, 2008.

[11] R. Panneton and X. Olny. Acoustical determination of the parameters governing viscous dissipation in porous media. *Journal of Acoustical Society of America*, 119(4):2027–2040, 2006.

[12] C. Perrot, R. Panneton, and X. Olny. Computation of the dynamic bulk modulus of acoustic foams. In *SAPEM*, ENTPE Lyon, 2005.

[13] B.H. Song, J.S. Bolton, and Y.J. Kang. Effect of circumferential edge constraint on the acoustical properties of glass fiber materials. *Journal of Acoustical Society of America*, 110(6):2902–2916, 2001.

[14] V. Tarnow. Dynamic measurements of the elastic constants of glass wool. *Journal of Acoustical Society of America*, 118(6):3672–3678, 2005.